

Magnetic Resonance Frequency Shift Caused by Nonuniform Field and Boundary Relaxation

Xiangdong Zhang,^{1,2} Jinbo Hu,¹ Da-Wu Xiao,¹ and Nan Zhao^{1,*}

¹Beijing Computational Science Research Center, Beijing 100193, People's Republic of China

²College of Physics and Optoelectronic Engineering, Shenzhen University, Shenzhen 518060, China

(Dated: April 26, 2024)

Magnetic field inhomogeneity is usually detrimental to magnetic resonance (MR) experiments. It is widely recognized that a nonuniform magnetic field can lead to an increase in the resonance line width, as well as a reduction in sensitivity and spectral resolution. However, nonuniform magnetic field can also cause shift in resonance frequency, which received far less attention. In this work, we investigate the frequency shift under arbitrary nonuniform magnetic field and boundary relaxation by applying perturbation theory to the Torrey equation. Several compact frequency shift formulas are reported. We find that the frequency shift is mainly determined by B_z distribution (rather than the transverse field components in previous study) and has important dependence on boundary relaxation. Furthermore, due to the difference of boundary relaxation and high order perturbation correction, this frequency shift is spin-species dependent, which implies a systematic error in many MR based precision measurements such as NMR gyroscope and comagnetometers. This insight provides a potential tool for understanding the unexplained isotope shifts in recent NMR gyroscope and new physics searching experiments that utilize comagnetometers. Finally, we propose a new tool for wall interaction research based on the frequency shift's dependency on boundary relaxation.

Introduction.—The nuclear magnetic resonance (NMR) technique has important applications in many fields, such as biochemistry [1, 2], medical imaging [3, 4], inertial navigation [5, 6], and new physics detection using comagnetometer [7–9]. For gas-phase NMR, the interaction between diffusion effect and nonuniform magnetic field has been a focus of research for decades. Nonuniform magnetic field contributes an extra relaxation rate to the diffusive nuclear spins, which is usually harmful to the precision of NMR experiment. Extensive works have been done to analyze this extra relaxation rate in various scenarios [10–20]. On the contrary, the frequency shift caused by nonuniform magnetic field is relatively underexplored. Unexpected spin-species dependent frequency shift [21] caused by nonuniform magnetic field can introduce significant systematic error in NMR based precision measurements that need to suppress main field fluctuation by comparing the resonance frequencies of different spins. Such measurements recently show great potential in the exploration of new physics, as illustrated in the works of Refs. [8, 22–29]. So, it is of great interest to understand how a nonuniform magnetic field affect the resonance frequency of spins.

Nonuniform magnetic field of different magnitude can result in significantly different behaviors. With small nonuniform field, the structure of free-induction decay (FID) spectrum is not changed, perturbation theory can be used to estimate the frequency shift. This region is called the fast diffusion area, meaning that the spins can diffuse throughout the whole cell before completely decayed. When the field inhomogeneity is large compared to diffusion speed, the FID spectrum can split due to the symmetry breaking of eigenmodes [14, 30]. This splitting phenomenon lies in the intermediate regime between fast and slow diffusion limit, and is closely related to the well known edge enhancement effect [31–34]. This work focus on the small nonuniform field limit, as most of the NMR based precision measurements lie in this region.

In an early work of Cates *et al.* [11], the frequency shift $\delta\omega$ of diffusive spins filled in a spherical container of radius R is derived by applying the second order perturbation theory on Torrey equation:

$$\delta\omega \approx \frac{\gamma R^2}{10B_0} \left(|\nabla B_x|^2 + |\nabla B_y|^2 \right), \quad (1)$$

where B_0 is the uniform main field along z direction and B_x, B_y are the transverse fields. This formula is valid for fast diffusion and high pressure limit. Similar results also presented in later works based on the Redfield theory [18, 35, 36]. Unfortunately, this formula requires the magnetic field to hold an odd-parity symmetry. If the odd-parity symmetry is broken, as in many practical experiments, this formula will underestimate the magnitude of the frequency shift.

On the other hand, Sheng *et al.* [37] analyzed the frequency shift from an arbitrary nonuniform field by numerical simulation. They expanded the nonuniform magnetic field using spherical harmonics and transformed the Torrey equation into a linear ODE system, which is suitable for numerical simulation. Through dimensional analysis, the frequency shift caused by a quadratic gradient field was found to be

$$\delta\omega \propto \frac{\gamma^3 G_2^3 R^{10}}{D^2}, \quad (2)$$

where D is the diffusion constant and G_2 is the strength of quadratic gradient. Due to the dependence on γ and D , this frequency shift will lead to a systematic error in ^3He - ^{129}Xe comagnetometer experiments [37]. The frequency shift Eq. (2) is actually a third order perturbation correction, coming from the nonuniform B_z distribution, whose effect is vanished in Eq. (1).

The boundary relaxation is another crucial factor that not well studied but can influence the resonance frequency by the interaction with nonuniform field. We find that the boundary condition λ , defined in Eq. (7), play a critical role in the first

order perturbation correction, and is the main source of systematic error for small cells.

In this work, we aim to investigate the frequency shift effect of a nonuniform magnetic field with arbitrary spatial distribution, and especially its interaction with boundary relaxation. The frequency shift for magnetic field without odd-parity symmetry behaves significantly different from Eq. (1). We also find that the boundary relaxation will lead to a frequency shift that is spin-species dependent due to the wall interaction mechanism difference of different spins. High order perturbation corrections are also spin-species dependent due to the difference of gyromagnetic ratio and diffusion constant. These corrections can introduce systematic errors in comagnetometer type measurements, and is fatal in new physics searching experiments where the absolute value of frequency ratio are of great concern. As a reference, systematic error for the rotation signal of an NMR gyroscope can as large as 10 μHz in typical experiment conditions (see Fig. 2). This insight can help explain the isotope shift effect [22, 38–41] in recent NMR gyroscope and new physics searching experiments. Furthermore, based on the derived systematic error formulas, a new method for wall relaxation measurement is proposed.

We will focus on the high pressure and fast diffusion limit, which is commonly satisfied in recent NMR based precision measurement experiments. The high pressure limit requires a large main field and small diffusion constant (i.e. $\gamma B_0 L^2/D \gg 1$ [18]), allowing the application of Rotating Wave Approximation (RWA) to the Torrey equation. The fast diffusion limit requires a slow relaxation rate compared to the diffusion speed (i.e. $DT_2/L^2 \gg 1$ [18]), so that the spin evolution can be well approximated by a single eigenmode and the effect of nonuniform magnetic field can be treated with perturbation theory. Weak boundary relaxation ($\lambda \ll 1$) is also assumed based on normal experiment condition.

Torrey Equation.—Use Xe nuclear spin as an example. In experiments utilizing spin-exchange optical pumping technique, such as NMR gyroscope and Rb-Xe comagnetometer, the diffusion of Xe nuclear spins can be described by the Bloch-Torrey equation [42]

$$\frac{\partial \mathbf{M}(\mathbf{r}, t)}{\partial t} = D\nabla^2 \mathbf{M}(\mathbf{r}, t) - \gamma_{\text{Xe}} \mathbf{B}(\mathbf{r}) \times \mathbf{M}(\mathbf{r}, t) - \Gamma_0 \cdot \mathbf{M}(\mathbf{r}, t) + R'_p [\mathbf{S}(\mathbf{r}) - \mathbf{M}(\mathbf{r}, t)], \quad (3)$$

where $\mathbf{M}(\mathbf{r}, t)$ is the Xe nuclear spin magnetization, D is the diffusion coefficient of Xe atoms, $\mathbf{\Omega}(\mathbf{r}) = \gamma_{\text{Xe}} \mathbf{B}(\mathbf{r})$ is the Larmor frequency in magnetic field $\mathbf{B}(\mathbf{r})$ with γ_{Xe} being the gyromagnetic ratio of Xe nuclear spins, $\Gamma_0 = \Gamma_{20}(\hat{x}\hat{x} + \hat{y}\hat{y}) + \Gamma_{10}\hat{z}\hat{z}$ is a tensor describing the transverse and longitudinal spin relaxation processes, and the last term arises from the spin-exchange pumping process between Xe and alkali atom spins, with R'_p the spin-exchange pumping rate. We assume that the alkali spins are polarized along the \hat{z} direction, i.e., $\mathbf{S}(\mathbf{r}) = S_z(\mathbf{r})\hat{z}$.

To further simplify Eq. (3), we assume that the magnetic field only has \hat{z} component (the effect of transverse component

can be estimated using Eq. (15)), i.e.,

$$\mathbf{B}(\mathbf{r}) = [B_0 + B_1(\mathbf{r})]\hat{z}, \quad (4)$$

with $|B_1(\mathbf{r})| \ll B_0$. The homogeneous field B_0 defines the main precession frequency $\Omega_0 = \gamma_{\text{Xe}} B_0$, while the inhomogeneous field $B_1(\mathbf{r})$, which may originate from the imperfection of the coils, the environmental stray fields, and the polarization field of the alkali atoms, can contribute spin relaxation and frequency shift.

With assumption Eq. (4), the transverse and longitudinal components of Eq. (3) are decoupled. The equation of motion of the transverse components $M_{\pm}(\mathbf{r}, t) \equiv M_x(\mathbf{r}, t) \pm iM_y(\mathbf{r}, t)$ is

$$\frac{\partial M_{\pm}(\mathbf{r}, t)}{\partial t} = [D\nabla^2 - \Gamma_{2c} \mp i\gamma_{\text{Xe}} B_z(\mathbf{r})] M_{\pm}(\mathbf{r}, t), \quad (5)$$

where $\Gamma_{2c} \equiv \Gamma_{20} + R'_p$, and $B_z(\mathbf{r}) \equiv B_0 + B_1(\mathbf{r})$. Below, we will focus on Eq. (5), which determines the FID behavior of Xe spins.

Boundary Condition.—The boundary condition of Eq. (5) is determined by the spin relaxation processes due to wall interaction. A perturbation treatment together with kinetic theory gives the following boundary condition of the Xe nuclear spin density matrix $\rho(\mathbf{r}, t)$ [43]

$$[\mathbf{n} \cdot \nabla \rho(\mathbf{r}, t) + \hat{\mu} \rho(\mathbf{r}, t)]|_{\mathbf{r} \in \partial V} = 0, \quad (6)$$

where ∂V is the boundary of solution domain V , \mathbf{n} is the normal vector of the boundary (pointing outward), and $\hat{\mu}$ is an operator reflecting the wall-interaction induced transitions between different components of the Xe spin polarization.

We replace the operator $\hat{\mu}$ with a constant number for simplification, leading to the following boundary condition:

$$\left(\mathbf{n} \cdot \nabla M_{\pm}(\mathbf{r}, t) + \frac{\lambda}{L} \cdot M_{\pm}(\mathbf{r}, t) \right)|_{\mathbf{r} \in \partial V} = 0, \quad (7)$$

where $\lambda \geq 0$ is a dimensionless constant describing the depolarization strength on the container wall and L is a linear size of V (e.g. the side length for cubic V or the radius for spherical V , the choice of L does not affect the physics). When $\lambda \rightarrow 0$, the boundary condition becomes $\mathbf{n} \cdot \nabla M_{\pm}(\mathbf{r}, t)|_{\mathbf{r} \in \partial V} = 0$, which represents an ideal surface without spin depolarization effect. In the opposite limit $\lambda \rightarrow \infty$, the boundary condition becomes $M_{\pm}(\mathbf{r}, t)|_{\mathbf{r} \in \partial V} = 0$, which means the spin magnetization is completely randomized at the wall. Compared with the Eq. (17) of Ref. [43], we have

$$\lambda \approx \frac{3L}{4\lambda_T} \xi_s^B, \quad \text{when } \xi_s^B \ll 1, \quad (8)$$

where λ_T is the mean free path of Xe atoms and $0 < \xi_s^B \ll 1$ represents the depolarization probability of Xe spins on the wall. For noble gases the depolarization probability is very small, $\xi_s^B \lesssim 10^{-7}$. Since λ_T and ξ_s^B are physical parameters that do not dependent on the size of V , the parameter λ is actually linearly scales with L , i.e., $\lambda \propto L$. The typical value of λ for RbH coated cell or uncoated Pyrex cell in an experimental

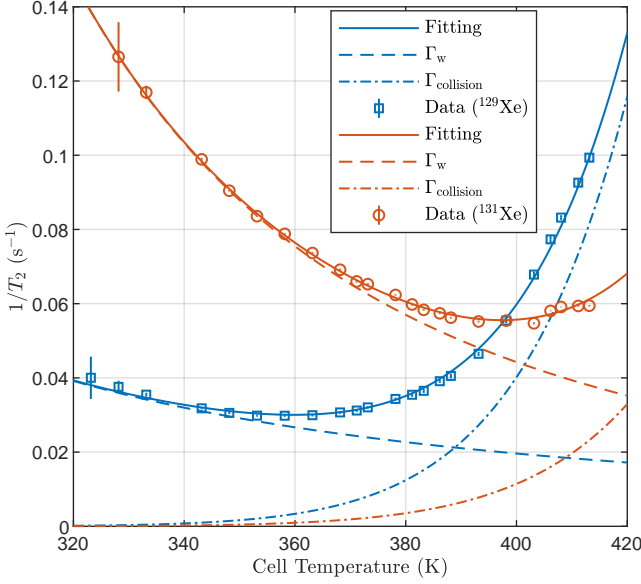


FIG. 1. A demo of Xe wall relaxation measurement. The measurement is performed on a RbH coated 8 mm cubic cell (Cell ID: CH7) containing 3.6 Torr ^{129}Xe , 35.6 Torr ^{131}Xe , 167 Torr N_2 , 6 Torr H_2 and a small droplet of Rb metal. The transverse relaxation rate of ^{129}Xe and ^{131}Xe is measured under various cell temperature using the experiment setup of Ref. [30]. Solid and dashed lines are fitting curves using the model in Sec. V of Supplemental Material [44]. The boundary conditions for ^{129}Xe and ^{131}Xe are estimated to be $\lambda_{129} = (5.3 \pm 2.0) \times 10^{-3}$ and $\lambda_{131} = (13.0 \pm 3.8) \times 10^{-3}$ using these fittings.

Rb-Xe comagnetometer system is approximately $10^{-3} \sim 10^{-2}$ for $L \approx 1$ cm cubic cells. Figure 1 shows an example of λ measurement experiment. The magnitude of λ is indeed small and has vast difference over different spin species. So, in the derivation below, the condition $\lambda \ll 1$ always holds, and we assume that λ is strongly spin-species dependent.

Perturbation Treatment.—The general solution of Eq. (5)

$$\begin{aligned}
 s_0 &= \underbrace{D\kappa_0^2 + \Gamma_{2c} + i\gamma_{\text{Xe}}B_0}_{0^{\text{th}} \text{ order}} + \underbrace{i\gamma_{\text{Xe}}b_{00}}_{1^{\text{st}} \text{ order}} + \underbrace{\gamma_{\text{Xe}}^2 \sum_{\alpha \neq 0} \frac{b_{0\alpha}b_{\alpha 0}}{D(\kappa_\alpha^2 - \kappa_0^2)}}_{2^{\text{nd}} \text{ order}} - \underbrace{i\gamma_{\text{Xe}}^3 \sum_{\alpha, \beta \neq 0} \frac{b_{0\alpha}b_{\alpha\beta}b_{\beta 0}}{D^2(\kappa_\alpha^2 - \kappa_0^2)(\kappa_\beta^2 - \kappa_0^2)}}_{3^{\text{rd}} \text{ order (a)}} + \underbrace{i\gamma_{\text{Xe}}^3 b_{00} \sum_{\alpha \neq 0} \frac{b_{0\alpha}b_{\alpha 0}}{D^2(\kappa_\alpha^2 - \kappa_0^2)^2}}_{3^{\text{rd}} \text{ order (b)}} \\
 &\equiv s_0^{(0)} + s_0^{(1)} + s_0^{(2)} + s_0^{(3)},
 \end{aligned} \tag{14}$$

where $s_0^{(k)}$ denotes the k^{th} order correction. As the perturbation matrix element $b_{\alpha\beta}$ is real, the 1st and 3rd order corrections are purely imaginary, which contributes to the frequency shift.

has the form

$$M_+(\mathbf{r}, t) = \sum_{\alpha} a_{\alpha} e^{-s_{\alpha} t} \Psi_{\alpha}(\mathbf{r}), \tag{9}$$

where $\{a_{\alpha}\}$ are expansion coefficients depending on initial state, $\{s_{\alpha}\}$ and $\{\Psi_{\alpha}(\mathbf{r})\}$ are the spatial eigenvalues and eigenmodes of Eq. (5). When the nonuniform magnetic field $B_1(\mathbf{r})$ is small, due to the fast decay rate of excited modes, usually only one mode is experimentally observable (fast diffusion limit). Thus, we have

$$M_+(\mathbf{r}, t) \approx a_0 e^{-s_0 t} \Psi_0(\mathbf{r}), \tag{10}$$

which describes the FID signal of Xe spins.

The eigen equation of Eq. (5) can write as

$$[\hat{H}_0 + \hat{H}_1(\mathbf{r})] \Psi_{\alpha}(\mathbf{r}) = -s_{\alpha} \Psi_{\alpha}(\mathbf{r}), \tag{11}$$

where $\hat{H}_0 \equiv D\nabla^2 - (i\gamma_{\text{Xe}}B_0 + \Gamma_{2c})$ and $\hat{H}_1 \equiv -i\gamma_{\text{Xe}}B_1(\mathbf{r})$.

Denote $\{\phi_{\alpha}(\mathbf{r}), \kappa_{\alpha}\}$ to be the eigen solution of \hat{H}_0 under boundary condition Eq. (7):

$$\nabla^2 \phi_{\alpha}(\mathbf{r}) = -\kappa_{\alpha}^2 \phi_{\alpha}(\mathbf{r}). \tag{12}$$

Then, we can calculate the matrix form of \hat{H}_0 and \hat{H}_1 under the orthonormalized basis $\{\phi_{\alpha}(\mathbf{r})\}$ and apply the results of non-degenerate time-independent perturbation theory, only to remember that \hat{H}_0 and \hat{H}_1 are non-Hermitian. H_0 is diagonal, and the matrix elements of H_1 are $(H_1)_{\alpha\beta} = -i\gamma_{\text{Xe}}b_{\alpha\beta}$ with $b_{\alpha\beta}$ being the $B_1(\mathbf{r})$ induced coupling between eigenmodes:

$$b_{\alpha\beta} \equiv \int_V \phi_{\alpha}(\mathbf{r}) B_1(\mathbf{r}) \phi_{\beta}(\mathbf{r}) d^3 \mathbf{r}. \tag{13}$$

Above, the Greek indices α, β may contain multiple integer indices, e.g. $\alpha = [mnp]$. The fundamental mode in Eq. (10), which has the slowest decay rate, is denoted using $\alpha = 0$ or $\beta = 0$.

We are particularly interested in the perturbation correction of the eigenvalue s_0 of the fundamental mode, which can be directly observed via the FID frequency shift and the spin decay rate. The eigenvalue of the fundamental mode, up to third order correction, is

The 2nd order corrections are real, which modifies the spin relaxation rate. The first order correction b_{00} is a weighted average of the inhomogeneous field $B_1(\mathbf{r})$. In the absence of

boundary relaxation ($\lambda = 0$), the weight $\phi_0(\mathbf{r})^2$ is constant, making b_{00} just a trivial average of $B_1(\mathbf{r})$. For $0 < \lambda \ll 1$, the boundary relaxation makes the fundamental mode $\phi_0(\mathbf{r})$ slightly different from uniform distribution, and the first order correction will have a small dependence on λ .

When the solution domain and $B_1(\mathbf{r})$ have parity symmetry, the 1st and 3rd order corrections above may vanish. Then, the effect of transverse magnetic field (B_x, B_y) is not negligible. In order to calculate the effect of transverse magnetic field, we can directly replace all the $\{b_{\alpha\beta}\}$ in Eq. (14) with the following $\{b_{\alpha\beta}^{(\text{tot})}\}$ (See Sec. I of the Supplemental Material [44]):

$$b_{\alpha\beta}^{(\text{tot})} \equiv b_{\alpha\beta} + \frac{\gamma_{\text{Xe}}}{2[\gamma_{\text{Xe}}B_0 - i(D\kappa_\beta^2 + \Gamma_{2c})]} \sum_\gamma b_{\alpha\gamma}^+ b_{\gamma\beta}^-, \quad (15)$$

$$b_{\alpha\beta}^\pm \equiv \int_V \phi_\alpha(\mathbf{r}) [B_x(\mathbf{r}) \pm iB_y(\mathbf{r})] \phi_\beta(\mathbf{r}) d^3\mathbf{r}.$$

For typical experiment condition, B_0 is much larger than B_1 , B_x , B_y and $(D\kappa_0^2 + \Gamma_{2c})/\gamma_{\text{Xe}}$. So, in Eq. (15), compared with B_1 , the effect of B_x is suppressed by a factor of B_x/B_0 (and the same for B_y). This validates the previous assumption Eq. (4). The effect of transverse magnetic field is important only when the contribution of B_1 vanishes due to symmetry reason (as shown below).

Frequency Shift from Gradient Field.—So far, we haven't specified the shape of solution domain V . Thus, the solutions above are applicable to arbitrary V . Now, let's consider a cubic domain

$$V = \{(x, y, z) | -L/2 \leq x, y, z \leq +L/2\}, \quad (16)$$

with L the cubic's side length. In Sec. II of the Supplemental Material [44], we find the eigenmodes in this cubic domain have a separable form

$$\phi_{mnp}(\mathbf{r}) = \phi_m(x)\phi_n(y)\phi_p(z), \quad (17)$$

where

$$\phi_p(z) = \frac{1}{N_p} \sin(\kappa_p z + \delta_p), \quad \delta_p = \frac{(p+1)\pi}{2}. \quad (18)$$

Obviously, $\phi_p(z)$ has parity: $\phi_p(z) = \phi_p(-z)$ for even p and $\phi_p(z) = -\phi_p(-z)$ for odd p . Using this symmetry, one can immediately derive that, for linear gradient field $B_1(\mathbf{r}) = G_1 \cdot z$, $b_{00} = 0$ and $b_{0\alpha} b_{\alpha\beta} b_{\beta 0} = 0, \forall \alpha, \beta \neq 0$. So, the frequency shift vanishes up to third order if we omit the effect of transverse magnetic field.

To count the transverse field, we note that a linear gradient field with axial symmetry should have the form

$$\mathbf{B} = G_1 \left[-\frac{1}{2}(x\hat{x} + y\hat{y}) + z\hat{z} \right]. \quad (19)$$

Following the calculation in Sec. III of the Supplemental Material [44], by using the $b_{\alpha\beta}^{(\text{tot})}$, we get the first order correction of frequency shift to be

$$\delta\omega^{(1)} \equiv -is_0^{(1)} \approx \frac{\gamma_{\text{Xe}}G_1^2L^2}{48B_0} \left(1 - \frac{2}{15}\lambda \right) + O(\lambda^2). \quad (20)$$

The λ^0 part of Eq. (20) has similar form with Eq. (1) by noting that $|\nabla B_x|^2 = |\nabla B_y|^2 = G_1^2/4$. Ref. [18] also obtained this formula for a cubic domain based on Redfield theory, but is twice as large as our result [45].

The second order correction, which contributes to relaxation rate, is

$$\frac{1}{T_2^G} \equiv s_0^{(2)} \approx \frac{\gamma_{\text{Xe}}^2 G_1^2 L^4}{120D} \left(1 - \frac{\lambda}{3} \right) + O(\lambda^2). \quad (21)$$

Equation (21) is derived using $b_{\alpha\beta}$, because the contribution from transverse field is negligible.

For an axial symmetric, quadratic gradient field

$$\mathbf{B} = G_2 \left[-xz\hat{x} - yz\hat{y} + z^2\hat{z} \right], \quad (22)$$

following the calculation in Sec. III of the Supplemental Material [44], the frequency shifts and relaxation rate are

$$\delta\omega^{(1)} \equiv -is_0^{(1)} \approx \frac{\gamma_{\text{Xe}}G_2L^2}{12} \left(1 - \frac{2}{15}\lambda \right) + O(\lambda^2), \quad (23)$$

$$\delta\omega^{(3)} \equiv -is_0^{(3)} \approx -\frac{\gamma_{\text{Xe}}^3 G_2^3 L^{10}}{D^2} \chi_1 (1 + \chi_2 \lambda) + O(\lambda^2), \quad (24)$$

$$\frac{1}{T_2^G} \equiv s_0^{(2)} \approx \frac{\gamma_{\text{Xe}}^2 G_2^2 L^6}{7560D} \left(1 - \frac{2}{15}\lambda \right) + O(\lambda^2), \quad (25)$$

where

$$\chi_1 \approx 6.68056 \times 10^{-8}, \quad \chi_2 \approx 0.646886. \quad (26)$$

Unlike the previously well known result Eq. (1), these two frequency shifts are determined by the distribution of longitudinal field $B_1(\mathbf{r})$ rather than transverse fields. They cannot be suppressed by a large B_0 and are sensitive to boundary relaxation. Transverse fields have much smaller effect due to the suppression factor B_x/B_0 . Comparing Eq.(24) and Eq. (2), the dimensional analysis result in Ref. [37] is actually a third order correction to the resonance frequency.

In NMR gyroscope [6] and comagnetometer [37] experiments, two different kinds of nuclear spins are used to compensate the fluctuation of main field B_0 . However, Eqs. (20), (23) and (24) show that nonuniform magnetic field will lead to frequency shifts depending on λ , γ and D , which can be different for different nuclear spins. These spin-species dependent frequency shifts may lead to imperfect compensation of magnetic field fluctuation. Following the analysis in Sec. IV of the Supplemental Material [44], Eqs. (20), (23) and (24) will respectively contribute systematic errors to the rotation signal of a NMR gyroscope as

$$\delta\Omega_{\text{rot}} \approx \frac{\lambda_{131} - \lambda_{129}}{L} \frac{\bar{\gamma}G_1^2L^3}{360B_0}, \quad (27)$$

$$\delta\Omega_{\text{rot}} \approx \frac{\lambda_{131} - \lambda_{129}}{L} \frac{\bar{\gamma}G_2L^3}{90}, \quad (28)$$

$$\delta\Omega_{\text{rot}} \approx -\chi_1 \left(\frac{\gamma_{129}^2}{D_{129}^2} - \frac{\gamma_{131}^2}{D_{131}^2} \right) \bar{\gamma}G_2^3L^{10}, \quad (29)$$

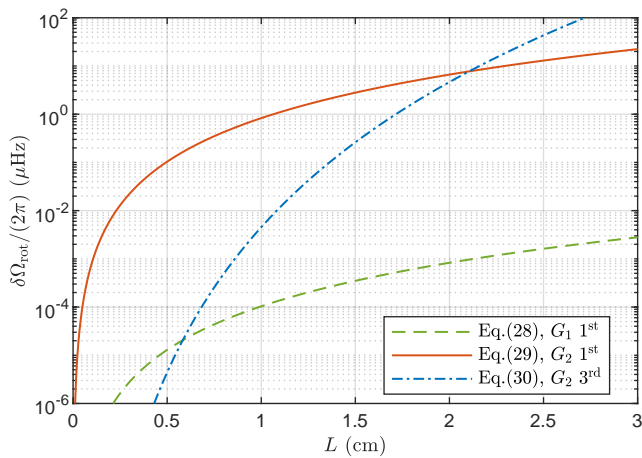


FIG. 2. The relative magnitude of different systematic errors. In the numerical calculation, $B_0 = 20000$ nT, $G_1 = 10$ nT/cm and $G_2 = 10$ nT/cm² are used. The values of λ and D are chosen to be the experimentally measured results presented in Sec. V of Supplemental Material [44].

where $\lambda_{129/131}$, $\gamma_{129/131}$ and $D_{129/131}$ are parameters for ^{129}Xe and ^{131}Xe spins respectively. $\bar{\gamma} \equiv \gamma_{129}\gamma_{131}/(\gamma_{131} - \gamma_{129})$. Systematic error of Eq. (29) was experimentally studied in Ref. [37] using ^3He - ^{129}Xe comagnetometer.

Figure 2 shows the magnitude of these systematic errors for various cell size. For small cell, first order correction dominates the systematic error. Matching the λ value of different spins helps reduce this systematic error. As cell size gets larger, third order (and higher order) correction become significant and finally blows up. A 2 cm cubic cell (usually used in new physics searching experiments) can gain systematic errors in 10 μHz order. These errors should play an important role in understanding the fundamental precision limit of NMR gyroscope and new physics detection based on comagnetometers. Our result can be used to explain the isotope shift effect observed in comagnetometer type experiments [22, 38–41] by noticing that the effective magnetic field of polarized Alkali atom spins has a highly nonuniform spatial distribution, leading to complex spin-species dependent frequency shifts.

Equations (27) and (28) convert the boundary condition λ into a frequency signal $\delta\Omega_{\text{rot}}$, thus can be used to measure the wall relaxation rate of nuclear spins. Compared to previous wall relaxation experiment which need to sweep cell temperature [43, 46–51], our new method is much faster and capable of real time monitoring the change of λ . The amplitude of $\delta\Omega_{\text{rot}}/(2\pi)$ in Eq. (28) is approximately 5 μHz (using typical values $\lambda \approx 10^{-3}$ and $\bar{\gamma}G_2L^2/(2\pi) \approx 0.5$ Hz), and should be easy to measure using state-of-art comagnetometer technique.

Conclusion.—The frequency shift formulas presented in this work show quite different behaviors with the previously well known formula Eq. (1) for magnetic field gradient. It turns out that Eq. (1) is a special case where magnetic field distribution and solution domain both have parity symmetry. The use of Eq. (1) may severely underestimate the actual fre-

quency shift caused by a nonuniform field.

It's notable that different spins have slightly different frequency shift. This deviation of frequency shift can introduce significant systematic error in comagnetometer experiments as well as other precision measurement experiments that rely on comparing the Larmor frequency of multiple kinds of spins. This systematic error could be one of the sources that limit the detection threshold of comagnetometer, which is a novel tool for dark matter searching [29], exotic interaction detection [23, 25, 28] and the verification of many other new physics models [7].

Equations (27) and (28) provide a new tool for the study of spin-wall interaction. Since frequency measurement is one of the most precise measurements, our new method has great advantages in precision and bandwidth. It should be a highly potential tool for spin-solid interaction research.

We thank Prof. Dong Sheng for giving advice to the overall structure of this article and for the assistance in producing the vapor cell used in Fig. 1. We also thank Dr. Sheng Zhang for his suggestions to improve the presentation of this article. This work is supported by NSFC (Grants No. U2030209, No. 12088101, and No. U2230402).

* nzhao@csrc.ac.cn

- [1] T. James, *Nuclear Magnetic Resonance in Biochemistry* (Academic Press, New York, 1975).
- [2] V. Mlynárik, *Analytical Biochemistry* **529**, 4 (2017).
- [3] R. G. Henderson, *Journal of the Royal Society of Medicine* **76**, 206 (1983).
- [4] W. R. Hendee, *Reviews of Modern Physics* **71**, S444 (1999).
- [5] D. Meyer and M. Larsen, *Gyroscopy and Navigation* **5**, 75 (2014).
- [6] T. G. Walker and M. S. Larsen, *Advances in Atomic, Molecular and Optical Physics* **65**, 373 (2016).
- [7] M. S. Safronova, D. Budker, D. DeMille, D. Kimball, A. Derevianko, and C. W. Clark, *Reviews of Modern Physics* **90**, 025008 (2018).
- [8] W. A. Terrano and M. V. Romalis, *Quantum Science and Technology* **7**, 014001 (2022).
- [9] D. F. Jackson Kimball, D. Budker, T. E. Chupp, A. A. Geraci, S. Kolkowitz, J. T. Singh, and A. O. Sushkov, *Physical Review A* **108**, 010101 (2023).
- [10] L. D. Schearer and G. K. Walters, *Physical Review* **139**, A1398 (1965).
- [11] G. D. Cates, S. R. Schaefer, and W. Happer, *Physical Review A* **37**, 2877 (1988).
- [12] G. D. Cates, D. J. White, T. R. Chien, S. R. Schaefer, and W. Happer, *Physical Review A* **38**, 5092 (1988).
- [13] D. D. McGregor, *Physical Review A* **41**, 2631 (1990).
- [14] S. D. Stoller, W. Happer, and F. J. Dyson, *Physical Review A* **44**, 7459 (1991).
- [15] L. J. Zielinski and P. N. Sen, *Journal of Magnetic Resonance* **147**, 95 (2000).
- [16] K. F. Zhao, M. Schaden, and Z. Wu, *Physical Review A* **78**, 034901 (2008).
- [17] R. Golub, R. M. Rohm, and C. M. Swank, *Physical Review A* **83**, 023402 (2011).

- [18] W. Zheng, H. Gao, J. G. Liu, Y. Zhang, Q. Ye, and C. Swank, *Physical Review A* **84**, 053411 (2011).
- [19] X. Zhan, C. Chen, Z. Wang, Q. Jiang, Y. Zhang, and H. Luo, *AIP Advances* **10**, 045002 (2020).
- [20] D.-Y. Lee, S. Lee, M. M. Kim, and S. H. Yim, *Physical Review A* **104**, 042819 (2021).
- [21] By saying a frequency shift is spin-species dependent, we mean the equivalent magnetic field of this frequency shift is different for different types of spin. Thus, this frequency shift cannot be cancelled together with the main field fluctuation in comagnetometer type experiment. ().
- [22] M. Bulatowicz, R. Griffith, M. Larsen, J. Mirijanian, C. B. Fu, E. Smith, W. M. Snow, H. Yan, and T. G. Walker, *Physical Review Letters* **111**, 102001 (2013).
- [23] K. Tullney, F. Allmendinger, M. Burghoff, W. Heil, S. Karpuk, W. Kilian, S. Knappe-Grüneberg, W. Müller, U. Schmidt, A. Schnabel, F. Seifert, Y. Sobolev, and L. Trahms, *Physical Review Letters* **111**, 100801 (2013).
- [24] S. Zimmer, *Search for a Permanent Electric Dipole Moment of ^{129}Xe with a He/Xe Clock-Comparison Experiment*, Ph.D. thesis, Johannes Gutenberg University, Mainz (2018).
- [25] J. Lee, A. Almasi, and M. Romalis, *Physical Review Letters* **120**, 161801 (2018).
- [26] N. Sachdeva, *A Measurement of the Permanent Electric Dipole Moment of ^{129}Xe* , Ph.D. thesis, University of Michigan (2019).
- [27] Y. K. Feng, D. H. Ning, S. B. Zhang, Z. T. Lu, and D. Sheng, *Physical Review Letters* **128**, 231803 (2022).
- [28] S.-B. Zhang, Z.-L. Ba, D.-H. Ning, N.-F. Zhai, Z.-T. Lu, and D. Sheng, *Physical Review Letters* **130**, 201401 (2023).
- [29] I. M. Bloch, R. Shaham, Y. Hochberg, E. Kufflik, T. Volansky, and O. Katz, *Nature Communications* **14**, 5784 (2023).
- [30] X. Zhang, J. Hu, and N. Zhao, *Physical Review Letters* **130**, 023201 (2023).
- [31] T. M. Deswriet, *Journal of Magnetic Resonance, Series B* **109**, 12 (1995).
- [32] B. Saam, N. Drukker, and W. Happer, *Chemical Physics Letters* **263**, 481 (1996).
- [33] Y. Q. Song, B. M. Goodson, B. Sheridan, T. M. De Swiet, and A. Pines, *Journal of Chemical Physics* **108**, 6233 (1998).
- [34] K. F. Zhao, M. Schaden, and Z. Wu, *Physical Review A* **81**, 042903 (2010).
- [35] M. Guigue, G. Pignol, R. Golub, and A. K. Petukhov, *Physical Review A* **90**, 013407 (2014).
- [36] J. Jeener, *Physical Review A* **91**, 013407 (2015).
- [37] D. Sheng, A. Kabcenell, and M. V. Romalis, *Physical Review Letters* **113**, 163002 (2014).
- [38] A. K. Vershovskii, A. S. Pazgalev, and V. I. Petrov, *Technical Physics Letters* **44**, 313 (2018).
- [39] V. I. Petrov, A. S. Pazgalev, and A. K. Vershovskii, *IEEE Sensors Journal* **20**, 760 (2020).
- [40] A. K. Vershovskii and V. I. Petrov, *Gyroscopy and Navigation* **11**, 198 (2020).
- [41] V. I. Petrov and A. K. Vershovskii, *Gyroscopy and Navigation* **13**, 82 (2022).
- [42] H. C. Torrey, *Physical Review* **104**, 563 (1956).
- [43] Z. Wu, *Reviews of Modern Physics* **93**, 035006 (2021).
- [44] (Reference to the Supplemental Material of This Work).
- [45] Eq. (20) of this work is half as large as Eq. (32) of Ref. [18]. It seems that there is a typo in Ref. [18]'s result. ().
- [46] C. H. Volk, T. M. Kwon, and J. G. Mark, *Physical Review A* **21**, 1549 (1980).
- [47] X. Zeng, E. Miron, W. Van Wijngaarden, D. Schreiber, and W. Happer, *Physics Letters A* **96**, 191 (1983).
- [48] A. T. Nicol, *Physical Review B* **29**, 2397 (1984).
- [49] Z. Wu, W. Happer, M. Kitano, and J. Daniels, *Physical Review A* **42**, 2774 (1990).
- [50] R. Butscher, G. Wäckerle, and M. Mehring, *The Journal of Chemical Physics* **100**, 6923 (1994).
- [51] B. Driehuys, G. D. Cates, and W. Happer, *Physical Review Letters* **74**, 4943 (1995).

Supplemental Material for Magnetic Resonance Frequency Shift Caused by Nonuniform Field and Boundary Relaxation

Xiangdong Zhang,^{1,2} Jinbo Hu,¹ Da-Wu Xiao,¹ and Nan Zhao^{1,*}

¹Beijing Computational Science Research Center, Beijing 100193, People's Republic of China

²College of Physics and Optoelectronic Engineering, Shenzhen University, Shenzhen 518060, China

(Dated: April 26, 2024)

CONTENTS

I. Perturbation Treatment of the 3D Torrey Equation	1
II. Unperturbed Eigenmodes in Cubic Domain	3
III. Frequency Shift Formulas for Gradient Fields	4
IV. Systematic Error of NMR Gyroscope	7
V. Experiment Measurement of Wall Relaxation Rate	7
References	8

(Note: In order not to introduce confusion, in this Supplemental Material, as well as maintext, subscript m, n, p will always represent a single integer index, while a Greek subscript such as α, β, γ represents multiple indices.)

I. PERTURBATION TREATMENT OF THE 3D TORREY EQUATION

This section considers the effect of transverse magnetic field in the presence of a large main field B_0 . Equation (3) of maintext can rewrite to the following form:

$$\begin{aligned}
\frac{\partial M_z}{\partial t} &= D\nabla^2 M_z - \frac{i}{2}\gamma_{Xe}(B_+M_- - B_-M_+) - \Gamma_{1c}M_z + R'_p S_z, \\
\frac{\partial M_+}{\partial t} &= D\nabla^2 M_+ - i\gamma_{Xe}(B_zM_+ - B_+M_z) - \Gamma_{2c}M_+, \\
\mathbf{B} &\equiv B_x(\mathbf{r})\hat{x} + B_y(\mathbf{r})\hat{y} + B_z(\mathbf{r})\hat{z}, \quad B_{\pm} \equiv B_x(\mathbf{r}) \pm iB_y(\mathbf{r}),
\end{aligned} \tag{S1}$$

with the boundary condition

$$\left(\mathbf{n} \cdot \nabla M_i(\mathbf{r}, t) + \frac{\lambda}{L} \cdot M_i(\mathbf{r}, t) \right) \Big|_{\mathbf{r} \in \partial V} = 0, \tag{S2}$$

where M_i stands for M_x, M_y or M_z . $\Gamma_{1c} \equiv \Gamma_{10} + R'_p, \Gamma_{2c} \equiv \Gamma_{20} + R'_p$. Suppose $B_z = B_0 + B_1(\mathbf{r})$ where B_0 is a large uniform main field and $B_1(\mathbf{r})$ is a small nonuniform field. Introduce the rotating frame with $\tilde{M}_{\pm} \equiv M_{\pm}e^{\pm i\gamma_{Xe}B_0t}$. Then, Eq. (S1) becomes

$$\begin{aligned}
\frac{\partial \tilde{M}_z}{\partial t} &= D\nabla^2 \tilde{M}_z - \frac{i}{2}\gamma_{Xe}(B_+\tilde{M}_-e^{+i\gamma_{Xe}B_0t} - B_-\tilde{M}_+e^{-i\gamma_{Xe}B_0t}) - \Gamma_{1c}\tilde{M}_z + R'_p S_z, \\
\frac{\partial \tilde{M}_+}{\partial t} &= D\nabla^2 \tilde{M}_+ - i\gamma_{Xe}B_1\tilde{M}_+ + i\gamma_{Xe}B_+M_z e^{+i\gamma_{Xe}B_0t} - \Gamma_{2c}\tilde{M}_+.
\end{aligned} \tag{S3}$$

In the rotating frame, the change of \tilde{M}_{\pm} and M_z should be slow compared to Larmor frequency $\gamma_{Xe}B_0$. So, in Eq. (S3), the high frequency terms which contain $e^{\pm i\gamma_{Xe}B_0t}$ factor can be directly ignored to the first approximation. This is called the Rotating

* nzhao@csrc.ac.cn

Wave Approximation (RWA), leading to the decoupling of M_z and \tilde{M}_\pm , and justifies the maintext's assumption of omitting the transverse component of magnetic field.

However, according to the first line of Eq. (S3), the solution of M_z can contain a small $e^{-i\gamma_{Xe}B_0t}$ component. Then, the $M_z e^{+i\gamma_{Xe}B_0t}$ term in the second line will generate a DC contribution which might have some effects to the solution of \tilde{M}_+ . So, let's consider the case when RWA is not directly applied to Eq. (S3).

Denote the eigenmodes of ∇^2 operator under the above boundary condition as

$$\nabla^2 \phi_\alpha(\mathbf{r}) = -\kappa_\alpha^2 \phi_\alpha(\mathbf{r}), \quad \int_V \phi_\alpha(\mathbf{r}) \phi_\beta(\mathbf{r}) d^3 \mathbf{r} = \delta_{\alpha\beta}. \quad (\text{S4})$$

Then, the solution of \mathbf{M} can be expanded as

$$M_z \equiv \sum_\alpha c_{z,\alpha}(t) \phi_\alpha(\mathbf{r}), \quad \tilde{M}_\pm \equiv \sum_\alpha \tilde{c}_{\pm,\alpha}(t) \phi_\alpha(\mathbf{r}), \quad \tilde{c}_{-,\alpha} = \tilde{c}_{+,\alpha}^*. \quad (\text{S5})$$

Using these expansions and the orthonormality of eigenmodes, one can transform Eq. (S3) into the following linear equation system of expansion coefficients:

$$\begin{aligned} \frac{dc_{z,\alpha}}{dt} &= -\left(D\kappa_\alpha^2 + \Gamma_{1c}\right) c_{z,\alpha} + R'_p d_{z,\alpha} - \frac{i}{2} \gamma_{Xe} \left(e^{+i\gamma_{Xe}B_0t} \sum_\beta b_{\alpha\beta}^+ \tilde{c}_{-\beta} - e^{-i\gamma_{Xe}B_0t} \sum_\beta b_{\alpha\beta}^- \tilde{c}_{+\beta} \right), \\ \frac{d\tilde{c}_{+,\alpha}}{dt} &= -\left(D\kappa_\alpha^2 + \Gamma_{2c}\right) \tilde{c}_{+,\alpha} - i\gamma_{Xe} \sum_\beta b_{\alpha\beta} \tilde{c}_{+\beta} + i\gamma_{Xe} e^{+i\gamma_{Xe}B_0t} \sum_\beta b_{\alpha\beta}^+ c_{z,\beta}. \end{aligned} \quad (\text{S6})$$

where

$$b_{\alpha\beta}^\pm \equiv \int_V \phi_\alpha(\mathbf{r}) B_\pm(\mathbf{r}) \phi_\beta(\mathbf{r}) d^3 \mathbf{r}, \quad b_{\alpha\beta} \equiv \int_V \phi_\alpha(\mathbf{r}) B_1(\mathbf{r}) \phi_\beta(\mathbf{r}) d^3 \mathbf{r}, \quad d_{z,\alpha} \equiv \int_V \phi_\alpha(\mathbf{r}) S_z(\mathbf{r}) d^3 \mathbf{r}. \quad (\text{S7})$$

Equation (S6) can be directly used in numerical simulation.

Integrate the $c_{z,\alpha}$ equation in Eq. (S6), one gets

$$\begin{aligned} c_{z,\alpha}(t) &= c_{z,\alpha}(0) + \int_0^t \left[R'_p d_{z,\alpha} - \left(D\kappa_\alpha^2 + \Gamma_{1c}\right) c_{z,\alpha}(t') \right] dt' \\ &\quad - \frac{i}{2} \gamma_{Xe} \sum_\beta \left[b_{\alpha\beta}^+ \left(\int_0^t e^{+i\gamma_{Xe}B_0t'} \tilde{c}_{-\beta}(t') dt' \right) - b_{\alpha\beta}^- \left(\int_0^t e^{-i\gamma_{Xe}B_0t'} \tilde{c}_{+\beta}(t') dt' \right) \right]. \end{aligned} \quad (\text{S8})$$

Based on the picture of Larmor precession and numerical simulation, we can safely assume that

$$\tilde{c}_{\pm,\alpha}(t) \approx \tilde{c}_{\pm,\alpha}(0) \exp(\mp i\omega_\alpha t - \Gamma_\alpha t), \quad (\text{S9})$$

where $\Gamma_\alpha \approx D\kappa_\alpha^2 + \Gamma_{2c}$ is the relaxation rate of $\phi_\alpha(\mathbf{r})$ mode, and ω_α is the frequency correction of this mode. Then, the integration above becomes

$$\int_0^t e^{\pm i\gamma_{Xe}B_0t'} \tilde{c}_{\mp,\beta}(t') dt' = \frac{c_{\mp,\beta}(0)}{\pm i(\gamma_{Xe}B_0 + \omega_\beta) - \Gamma_\beta} \left[e^{\pm i(\gamma_{Xe}B_0 + \omega_\beta)t - \Gamma_\beta t} - 1 \right]. \quad (\text{S10})$$

Insert Eqs. (S8) and (S10) into the $\tilde{c}_{+,\alpha}$ equation of Eq. (S6). Noticing that $|\omega_\beta| \ll |\gamma_{Xe}B_0|$, we can use RWA, ignoring all the terms with $e^{+i\gamma_{Xe}B_0t}$ or $e^{+i(2\gamma_{Xe}B_0 + \omega_\beta)t}$ factor. Finally, we get

$$\begin{aligned} \frac{d\tilde{c}_{+,\alpha}}{dt} &\approx -\left(D\kappa_\alpha^2 + \Gamma_{2c}\right) \tilde{c}_{+,\alpha} - i\gamma_{Xe} \sum_\beta b_{\alpha\beta} \tilde{c}_{+\beta} + \frac{\gamma_{Xe}^2}{2} \sum_{\beta,\gamma} \frac{b_{\alpha\gamma}^+ b_{\gamma\beta}^- \tilde{c}_{+\beta}}{\Gamma_\beta + i(\gamma_{Xe}B_0 + \omega_\beta)} \\ &\approx -\left(D\kappa_\alpha^2 + \Gamma_{2c}\right) \tilde{c}_{+,\alpha} - i\gamma_{Xe} \sum_\beta b_{\alpha\beta}^{(\text{tot})} \tilde{c}_{+\beta}, \end{aligned} \quad (\text{S11})$$

where

$$b_{\alpha\beta}^{(\text{tot})} \equiv b_{\alpha\beta} + \frac{\gamma_{Xe}}{2[\gamma_{Xe}B_0 - i(D\kappa_\beta^2 + \Gamma_{2c})]} \sum_\gamma b_{\alpha\gamma}^+ b_{\gamma\beta}^-. \quad (\text{S12})$$

If we directly apply RWA to Eq. (S3), which means ignoring all the effects of B_x and B_y , then Eq. (S11) becomes

$$\frac{d\tilde{c}_{+\alpha}}{dt} \approx -\left(D\kappa_\alpha^2 + \Gamma_{2c}\right)\tilde{c}_{+\alpha} - i\gamma_{Xe} \sum_{\beta} b_{\alpha\beta}\tilde{c}_{+\beta}, \quad (\text{S13})$$

which is equivalent to the eigen equation (11) in maintext. Comparing Eq. (S11) and (S13), it's easy to see that, to account the leading order effect of B_x and B_y , we just need to replace $\{b_{\alpha\beta}\}$ in Eq. (14) of maintext with $\{b_{\alpha\beta}^{(\text{tot})}\}$. Since the main field B_0 is much larger than nonuniform field B_1 , B_x and B_y , $b_{\alpha\beta}^{(\text{tot})}$ is dominated by $b_{\alpha\beta}$. The effect of $B_{x/y}$ is suppressed by a factor $B_{x/y}/B_0$ compared with B_1 . Also, the imaginary part of $b_{\alpha\beta}^{(\text{tot})}$ should be much smaller than its real part.

II. UNPERTURBED EIGENMODES IN CUBIC DOMAIN

This section will derive the eigenmodes and eigenvalues of Torrey equation in a cubic domain of the form Eq. (16) in maintext. Consider the following eigen equation:

$$D\nabla^2\phi_{mnp} - (i\gamma_{Xe}B_0 + \Gamma_{2c})\phi_{mnp} = -s_{mnp}^{(0)}\phi_{mnp}, \quad (\text{S14})$$

where $-s_{mnp}^{(0)}$ is the eigenvalue of the eigenmode $\phi_{mnp}(\mathbf{r})$.

The eigenmodes $\{\phi_{mnp}(\mathbf{r})\}$ of Eq. (S14) can be written in a factorized form of

$$\phi_{mnp}(\mathbf{r}) = \phi_m(x)\phi_n(y)\phi_p(z), \quad (\text{S15})$$

where m , n and p are non-negative integers labelling the eigenmodes in the x , y and z directions, respectively. It's easy to check that the 1D eigenmodes have the form

$$\phi_p(z) = \frac{1}{\mathcal{N}_p} \sin(\kappa_p z + \delta_p), \quad (\text{S16})$$

where \mathcal{N}_p is normalization factor, and κ_p and δ_p are real numbers determined by the boundary condition Eq. (7) in maintext. The wave numbers κ_p are the solutions of the transcendental equation

$$\tan(\kappa_p L) = \frac{2\lambda\kappa_p L}{\kappa_p^2 L^2 - \lambda^2}, \quad (\text{S17})$$

and the phase shifts are determined by

$$\tan\left(\delta_p - \frac{\kappa_p L}{2}\right) = \frac{\kappa_p L}{\lambda}. \quad (\text{S18})$$

Using the normalization condition $\int \phi_p^2(z) dz = 1$, the normalization factor is

$$\mathcal{N}_p = \sqrt{\frac{L}{2} + \frac{\lambda L}{\kappa_p^2 L^2 + \lambda^2}}. \quad (\text{S19})$$

The eigenvalues corresponding to $\phi_{mnp}(\mathbf{r})$ are

$$s_{mnp}^{(0)} = D\kappa_{mnp}^2 + \Gamma_{2c} + i\gamma_{Xe}B_0, \quad (\text{S20})$$

where $\kappa_{mnp}^2 \equiv \kappa_m^2 + \kappa_n^2 + \kappa_p^2$. The real part of the eigenvalue, $\Gamma_2 = D\kappa_{mnp}^2 + \Gamma_{2c}$, is the decay rate of the eigenmode $\phi_{mnp}(\mathbf{r})$, and the imaginary part, $\gamma_{Xe}B_0$, is the spin precession frequency in the uniform magnetic field B_0 . The superscript of $s_{mnp}^{(0)}$ represents that this is the 0th order correction of the perturbation solution presented in Eq. (14) of maintext.

Figure S1 gives the numerical solutions of κ_p for various λ values. To reveal the underlying physics of the wall-relaxation, we expand the tangent function in Eq. (S17) in the neighborhood of $\kappa_p L = p\pi$, and find the solution of wave number in the limit of $\lambda \ll 1$ to be

$$\kappa_p \approx \begin{cases} \frac{\sqrt{2\lambda}}{L} & , p = 0 \\ \frac{p\pi}{L} + \frac{2\lambda}{p\pi L} \approx \frac{p\pi}{L} & , p = 1, 2, \dots \end{cases}. \quad (\text{S21})$$

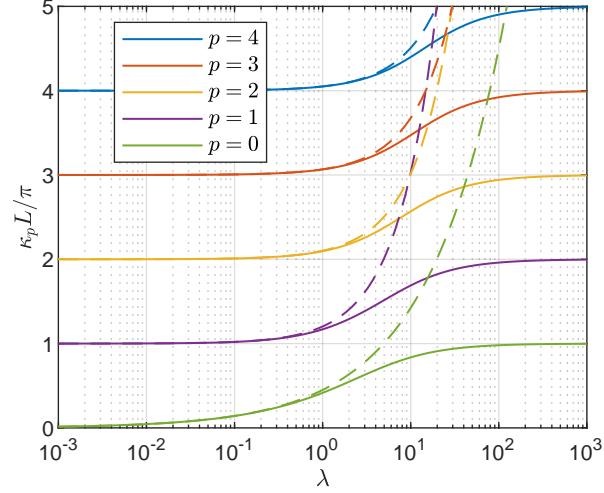


FIG. S1. The value of κ_p for various λ . The solid lines are the exact value calculated from numerical method. The dashed lines are the approximation value calculated from Eq. (S21).

The exact solution of δ_p (without assuming $\lambda \ll 1$) is

$$\delta_p = \frac{(p+1)\pi}{2}. \quad (\text{S22})$$

For the fundamental mode ($m = n = p = 0$), the wall-interaction contributes a relaxation rate through diffusion:

$$\Gamma_{000} \equiv D\kappa_{000}^2 \approx 6\lambda \frac{D}{L^2}. \quad (\text{S23})$$

For the excited modes ($[m, n, p] \neq [0, 0, 0]$), the relaxation rate due to spin diffusion is

$$\Gamma_{mnp} \equiv D\kappa_{mnp}^2 \approx (m^2 + n^2 + p^2)\pi^2 \frac{D}{L^2}. \quad (\text{S24})$$

As $\lambda \lesssim 10^{-2}$, even for the lowest excited modes (with $m^2 + n^2 + p^2 = 1$), the decay rate is much faster than the fundamental mode, i.e., $\Gamma_{mnp} \gg \Gamma_{000}$.

In the $\lambda \ll 1$ limit, $\phi_p(z)$ are approximately

$$\begin{aligned} \phi_0(z) &\approx \frac{1 - \lambda z^2/L^2}{\sqrt{L(1 - \lambda/6 + \lambda^2/80)}} \\ \phi_p(z) &\approx \begin{cases} \frac{1}{N_p} \sin \left[\left(\frac{p\pi}{L} + \frac{2\lambda}{p\pi L} \right) z \right], & p \text{ is odd} \\ \frac{1}{N_p} \cos \left[\left(\frac{p\pi}{L} + \frac{2\lambda}{p\pi L} \right) z \right], & p \text{ is even} \end{cases}, p > 0. \end{aligned} \quad (\text{S25})$$

III. FREQUENCY SHIFT FORMULAS FOR GRADIENT FIELDS

In this section, we calculate the frequency shift formulas for several simple forms of nonuniform magnetic field. Let's first consider a linear gradient field $B_z = B_0 + G_1 \cdot z$. Since a real magnetic field should obey the Gauss law, if we assume axial symmetry, magnetic field should have the following distribution:

$$\mathbf{B}(\mathbf{r}) = G_1 \left[-\frac{1}{2}(x\hat{x} + y\hat{y}) + z\hat{z} \right] + B_0\hat{z}. \quad (\text{S26})$$

The first order term b_{00} is zero, for the reason that $G_1 z$ is odd function and $\phi_0(z)$ in Eq. (S25) is even function. So, the first order frequency shift of a linear gradient field is mainly contributed from transverse components. We need to calculate the

$b_{00}^{(\text{tot})}$ in Eq. (S12). Let's first calculate $b_{0\alpha}^{\pm}$ using the definition Eq. (S7). According to the parity of the approximate eigenmode expressions in Eq. (S25), $b_{0\alpha}^{\pm}$ is nonzero only when $\alpha = [2p - 1, 0, 0]$ or $\alpha = [0, 2p - 1, 0]$, $p \geq 1$. Thus, we have

$$\begin{aligned} b_{0,[2p-1,0,0]}^{\pm} &= -\frac{G_1}{2} \int_{-L/2}^{+L/2} x \phi_0(x) \phi_{2p-1}(x) dx \\ &\approx (-1)^p \frac{\sqrt{2}G_1L}{(2p-1)^2\pi^2} \left\{ 1 - \left[\frac{1}{6} - \frac{1}{(2p-1)^2\pi^2} \right] \lambda \right\} + O(\lambda^2), \end{aligned} \quad (\text{S27})$$

$$\begin{aligned} b_{0,[0,2p-1,0]}^{\pm} &= -\frac{G_1}{2} \int_{-L/2}^{+L/2} (\pm iy) \phi_0(y) \phi_{2p-1}(y) dy \\ &\approx \pm i(-1)^p \frac{\sqrt{2}G_1L}{(2p-1)^2\pi^2} \left\{ 1 - \left[\frac{1}{6} - \frac{1}{(2p-1)^2\pi^2} \right] \lambda \right\} + O(\lambda^2). \end{aligned} \quad (\text{S28})$$

Above, we use Eq. (S25) as the approximate expressions of eigenmodes, and expand the result around $\lambda = 0$. Combining them together, we have

$$\begin{aligned} \sum_{\alpha} b_{0\alpha}^+ b_{\alpha 0}^- &= \sum_{p=1}^{\infty} (b_{0,[2p-1,0,0]}^+ b_{0,[2p-1,0,0]}^- + b_{0,[0,2p-1,0]}^+ b_{0,[0,2p-1,0]}^-) \\ &\approx 2 \sum_{p=1}^{\infty} \left(\frac{\sqrt{2}G_1L}{(2p-1)^2\pi^2} \left\{ 1 - \left[\frac{1}{6} - \frac{1}{(2p-1)^2\pi^2} \right] \lambda \right\} \right)^2 \\ &\approx \frac{G_1^2 L^2}{24} \left(1 - \frac{2}{15} \lambda \right) + O(\lambda^2) \end{aligned} \quad (\text{S29})$$

The first order frequency shift is:

$$-i s_0^{(1)} = \gamma_{\text{Xe}} b_{00}^{(\text{tot})} \approx \gamma_{\text{Xe}} \frac{\sum_{\alpha} b_{0\alpha}^+ b_{\alpha 0}^-}{2B_0} \approx \frac{\gamma_{\text{Xe}} G_1^2 L^2}{48B_0} \left(1 - \frac{2}{15} \lambda \right) + O(\lambda^2). \quad (\text{S30})$$

Second order correction mainly consists of the contribution from longitudinal component. Due to symmetry reason, $b_{0\alpha}$ is nonzero only when $\alpha = [0, 0, 2p - 1]$, $p \geq 1$. Using the approximate eigenmode in Eq. (S25), we have

$$\begin{aligned} b_{0,[0,0,2p-1]} &= G_1 \int_{-L/2}^{+L/2} z \phi_0(z) \phi_{2p-1}(z) dz \\ &\approx (-1)^{p+1} \frac{2\sqrt{2}G_1L}{(2p-1)^2\pi^2} \left\{ 1 - \left[\frac{1}{6} - \frac{1}{(2p-1)^2\pi^2} \right] \lambda \right\} + O(\lambda^2) \end{aligned} \quad (\text{S31})$$

The result above is a Taylor expansion around $\lambda = 0$. The second order correction is

$$\begin{aligned} s_0^{(2)} &= \frac{\gamma_{\text{Xe}}^2 L^2}{D} \sum_{p=1}^{\infty} \frac{(b_{0,[0,0,2p-1]})^2}{\left[(2p-1)\pi + \frac{2\lambda}{(2p-1)\pi} \right]^2 - 2\lambda} \\ &\approx \frac{\gamma_{\text{Xe}}^2 L^2}{D} \sum_{p=1}^{\infty} \frac{8G_1^2 L^2}{(2p-1)^6 \pi^6} \left(1 - \frac{\lambda}{3} \right) \\ &= \frac{\gamma_{\text{Xe}}^2 G_1^2 L^4}{120D} \left(1 - \frac{\lambda}{3} \right) + O(\lambda^2) \end{aligned} \quad (\text{S32})$$

For quadratic gradient field, if assume axial symmetry, the spatial distribution should be

$$\mathbf{B} = G_2 \left[-xz\hat{x} - yz\hat{y} + z^2\hat{z} \right] + B_0\hat{z}. \quad (\text{S33})$$

First order correction can be calculated directly using the approximate eigenmode in Eq. (S25):

$$b_{00} = G_2 \int_{-\frac{L}{2}}^{+\frac{L}{2}} z^2 \phi_0(z) \phi_0(z) dz \approx \frac{G_2 L^2}{12} \left(1 - \frac{2}{15} \lambda \right) + O(\lambda^2). \quad (\text{S34})$$

The calculation of second order correction is similar to linear gradient field. Due to symmetry reason, $b_{0\alpha}$ is nonzero only when $\alpha = [0, 0, 2p]$, $p \geq 1$. Using the approximate eigenmode in Eq. (S25), we have

$$\begin{aligned} b_{0,[0,0,2p]} &= G_2 \int_{-L/2}^{+L/2} z^2 \phi_0(z) \phi_{2p}(z) dz \\ &\approx (-1)^p \frac{G_2 L^2}{\sqrt{2} p^2 \pi^2} \left[1 - \left(\frac{1}{6} - \frac{5}{4p^2 \pi^2} \right) \lambda \right] + O(\lambda^2) \end{aligned} \quad (\text{S35})$$

The second order correction is

$$\begin{aligned} s_0^{(2)} &= \frac{\gamma_{Xe}^2 L^2}{D} \sum_{p=1}^{\infty} \frac{(b_{0,[0,0,2p]})^2}{\left[2p\pi + \frac{2\lambda}{2p\pi} \right]^2 - 2\lambda} \\ &\approx \frac{\gamma_{Xe}^2 L^2}{D} \sum_{p=1}^{\infty} \frac{G_2^2 L^4}{8p^6 \pi^6} \left[1 - \left(\frac{1}{3} - \frac{2}{p^2 \pi^2} \right) \lambda \right] \\ &= \frac{\gamma_{Xe}^2 G_2^2 L^6}{7560D} \left(1 - \frac{2}{15} \lambda \right) + O(\lambda^2) \end{aligned} \quad (\text{S36})$$

The calculation of third order correction is a bit complicated. The calculation of $s_0^{(3b)}$ term is similar to $s_0^{(2)}$:

$$\begin{aligned} s_0^{(3b)} &\approx i \frac{\gamma_{Xe}^3}{D^2} L^4 b_{00} \sum_{p=1}^{\infty} \frac{(b_{0,[0,0,2p]})^2}{\left[\left(2p\pi + \frac{2\lambda}{2p\pi} \right)^2 - 2\lambda \right]^2} \\ &\approx i \frac{\gamma_{Xe}^3 G_2^3 L^{10}}{3628800D^2} \left(1 - \frac{52}{165} \lambda \right) + O(\lambda^2) \end{aligned} \quad (\text{S37})$$

When calculating $s_0^{(3a)}$, we need the matrix element $b_{\alpha\beta}$. Due to symmetry reason, only when $\alpha = [0, 0, 2p]$, $\beta = [0, 0, 2n]$, the product $b_{0\alpha} b_{\alpha\beta} b_{\beta 0}$ in the numerator of $s_0^{(3a)}$ is nonzero. Using the approximate eigenmode in Eq. (S25), we have

$$\begin{aligned} b_{\alpha\beta} &= G_2 \int_{-L/2}^{+L/2} z^2 \phi_{2p}(z) \phi_{2n}(z) dz, \quad \alpha = [0, 0, 2p], \beta = [0, 0, 2n], n, p > 0 \\ &\approx \begin{cases} \frac{(-1)^{n+p} G_2 L^2 (n^2 + p^2)}{(n^2 - p^2)^2 \pi^2} \left[1 - \frac{n^4 - 10n^2 p^2 + p^4}{4n^2 p^2 (n^2 + p^2) \pi^2} \lambda \right], & p \neq n \\ \frac{G_2 L^2}{24} \left(2 + \frac{3}{p^2 \pi^2} \right) \left[1 + \frac{2p^2 \pi^2 - 6}{p^2 \pi^2 (2p^2 \pi^2 + 3)} \lambda \right], & p = n \end{cases} \end{aligned} \quad (\text{S38})$$

The result above is Taylor expanded near $\lambda = 0$. According Eq. (14) of maintext, we have

$$s_0^{(3a)} \approx -i \frac{\gamma_{Xe}^3}{D^2} L^4 \sum_{n=1}^{\infty} \sum_{p=1}^{\infty} \frac{b_{0,[0,0,2p]} b_{[0,0,2p],[0,0,2n]} b_{0,[0,0,2n]}}{\left[\left(2p\pi + \frac{2\lambda}{2p\pi} \right)^2 - 2\lambda \right] \left[\left(2n\pi + \frac{2\lambda}{2n\pi} \right)^2 - 2\lambda \right]} \quad (\text{S39})$$

Taylor expand the above formula at $\lambda = 0$ (up to first order), we get

$$s_0^{(3a)} \approx -i \frac{\gamma_{Xe}^3 G_2^3 L^{10}}{16D^2 \pi^{10}} \left[\left(1 - \frac{\lambda}{3} \right) \mathcal{S}_1 + \frac{\lambda}{2\pi^2} \mathcal{S}_2 \right] - i \frac{19\gamma_{Xe}^3 G_2^3 L^{10}}{59875200D^2} \left(1 - \frac{659}{5460} \lambda \right) + O(\lambda^2) \quad (\text{S40})$$

where

$$\mathcal{S}_1 \equiv \sum_{n=1}^{+\infty} \sum_{p=1}^{n-1} \frac{n^2 + p^2}{n^4 p^4 (n^2 - p^2)^2} \approx 0.0375373, \quad (\text{S41})$$

$$\mathcal{S}_2 \equiv \sum_{n=1}^{+\infty} \sum_{p=1}^{n-1} \frac{n^4 + 8n^2 p^2 + p^4}{n^6 p^6 (n^2 - p^2)^2} \approx 0.0892948. \quad (\text{S42})$$

TABLE S1. Fitting result of Fig. 1 in maintext.

	c_1 (10^{-15} cm ³ /s)	c_2 (10^{-3} s ⁻¹)	\bar{E} (meV)	Γ_w (s ⁻¹)@110°C
¹²⁹ Xe	1.343 ± 0.021	1.23 ± 0.34	95.4 ± 8.6	0.0222 ± 0.0084
¹³¹ Xe	0.382 ± 0.028	0.363 ± 0.075	165.6 ± 6.4	0.055 ± 0.015

Summing $s_0^{(3a)}$ and $s_0^{(3b)}$ together, we finally get the third order correction:

$$\begin{aligned}
s_0^{(3)} &\approx -i \frac{\gamma_{\text{Xe}}^3 G_2^3 L^{10}}{D^2} \chi_1 (1 + \chi_2 \lambda) + O(\lambda^2), \\
\chi_1 &\equiv \frac{S_1}{16\pi^{10}} + \frac{1}{23950080} \approx 6.68056 \times 10^{-8}, \\
\chi_2 &\equiv \left(\frac{15871}{326918592000} - \frac{S_1}{48\pi^{10}} + \frac{S_2}{32\pi^{12}} \right) / \chi_1 \approx 0.646886.
\end{aligned} \tag{S43}$$

IV. SYSTEMATIC ERROR OF NMR GYROSCOPE

In NMR gyroscope experiment, one often simultaneously measure the Larmor precession frequency of both ¹²⁹Xe and ¹³¹Xe nuclear spin. The Larmor frequencies of two Xe isotopes are

$$\omega_u = -\gamma_u(B_0 + \delta B_u) - \Omega_{\text{rot}}, \tag{S44}$$

where $u = 129$ or 131 , and $\delta B_u \equiv \mathfrak{J}[s_0]/\gamma_u - B_0$ is the frequency shift caused by nonuniform field. Ω_{rot} is the laboratory reference frame's rotation angular velocity along \hat{z} direction.

One usually estimates the rotation speed by the following estimator [1]:

$$\Omega_{\text{rot}}^{(2\omega)} \equiv \frac{|R_0 \omega_{131}| - |\omega_{129}|}{1 + |R_0|} = \text{sgn}[B_0] \left(\Omega_{\text{rot}} + \frac{\gamma_{129}}{1 + |R_0|} b_A \right), \tag{S45}$$

where $b_A \equiv \delta B_{129} - \delta B_{131}$ is called the differential field, and $R_0 \equiv \gamma_{129}/\gamma_{131} \approx -3.373417$. Obviously, this estimator introduces a systematic error proportional to b_A . Utilizing the frequency shift formulas derived in the above section, it's straight forward to get the Eqs. (27), (28) and (29) of maintext.

V. EXPERIMENT MEASUREMENT OF WALL RELAXATION RATE

According to Ref. [2, 3], the transverse relaxation rate of Xe spins mainly consists of two parts:

$$\frac{1}{T_2} = \underbrace{c_1 n_{\text{Rb}}(T)}_{\Gamma_{\text{collision}}} + \underbrace{c_2 \exp\left(\frac{\bar{E}}{k_B T}\right)}_{\Gamma_w}, \tag{S46}$$

where T is the cell temperature in degrees kelvin, $n_{\text{Rb}}(T)$ is the Rb atom number density, \bar{E} is a characteristic energy, k_B is the Boltzmann's constant, and c_1, c_2 are constant coefficients. $\Gamma_{\text{collision}}$ arises from the spin exchange collisions between Xe and Rb atoms and is proportional to Rb density. Γ_w comes from the wall interaction, which depends on cell temperature via an Arrhenius factor.

The solid lines in Fig. 1 of maintext is fitted curves using model Eq. (S46), with c_1, c_2, \bar{E} the fitting parameters. Rb density $n_{\text{Rb}}(T)$ is calculated using the Rb vapor-pressure formula Eq. (1) in Ref. [4] (also see Ref. [5]) together with the Ideal Gas Law. The fitting result is shown in Tab. S1. Quadrupole splitting of ¹³¹Xe is not observed in the experiment of Fig. 1 in maintext.

From Eq. (14) of maintext, the relaxation rate contributed from boundary condition is $\Gamma_w = D\kappa_0^2$. Thus, for cubic cell, using the solution in Sec.II, we can estimate the value of λ by Γ_w :

$$\Gamma_w = \frac{6\lambda D}{L^2}. \tag{S47}$$

The diffusion constant can be measured using the method described in Sec. II D of Ref. [1]’s Supplemental Material. The result is $D_{129} = D_{131} = (0.45 \pm 0.03) \text{ cm}^2/\text{s}$. The inner side length of cell is $L = (0.80 \pm 0.01) \text{ cm}$. Using these parameters, we get the boundary condition at 110°C to be $\lambda_{129} = (5.3 \pm 2.0) \times 10^{-3}$ and $\lambda_{131} = (13.0 \pm 3.8) \times 10^{-3}$.

- [1] X. Zhang, J. Hu, and N. Zhao, *Physical Review Letters* **130**, 023201 (2023).
- [2] C. H. Volk, T. M. Kwon, J. G. Mark, Y. B. Kim, and J. C. Woo, *Physical Review Letters* **44**, 136 (1980).
- [3] R. Butscher, G. Wäckerle, and M. Mehring, *The Journal of Chemical Physics* **100**, 6923 (1994).
- [4] D. A. Steck, *Rubidium 85 D Line Data* (2021).
- [5] C. B. Alcock, V. P. Itkin, and M. K. Horrigan, *Canadian Metallurgical Quarterly* **23**, 309 (1984).